Generator Coordinate Method Calculations for Ground and First Excited Collective States in ^{4}He, ^{16}O and ^{40}Ca Nuclei

M.V. Ivanov, A.N. Antonov, M.K. Gaidarov

Institute of Nuclear Research and Nuclear Energy, Bulgarian Academy of Sciences, Sofia 1784, Bulgaria

The main characteristics of the ground and, in particular, the first excited monopole state in the ^{4}He, ^{16}O and ^{40}Ca nuclei are studied within the generator coordinate method using Skyrme-type effective forces and three construction potentials, namely the harmonic-oscillator, the square-well and Woods-Saxon potentials. Calculations of density distributions, radii, nucleon momentum distributions, natural orbitals, occupation numbers and depletions of the Fermi sea, as well as of pair density and momentum distributions are carried out. A comparison of these quantities for both ground and first excited monopole states with the available empirical data and with the results of other theoretical methods are given and discussed in detail.

PACS number(s): 21.60.-n, 21.10.-k, 21.10.Re, 27.10.-h, 27.20.+n, 27.40.+z

I. INTRODUCTION

The study of nucleon-nucleon correlation effects is important part of the contemporary nuclear physics [1,2]. The basic idea of the independent particle models (IPM) consists in the assumption that nucleons move independently in a mean field created by the same nucleons. Consequently, each coherent motion of the nucleons creates changes in the mean field. The Hartree-Fock approximation accounts only partially for the dynamic nucleon correlations. There exist many experimental data (see e.g. the review in [2]) showing that the IPM are unable to describe basic nuclear characteristics. For instance, the nucleon momentum and density distributions in nuclei cannot be reproduced simultaneously [3,4]. This is also the case with the occupation numbers, the hole-state spectral functions, with characteristics of nuclear reactions and others [1,2,5–7]. This imposes the development of correlation methods going beyond the limits of the mean-field approximation (MFA) which account for nucleon-nucleon correlations (see e.g. [2]). This can be reached by extending the class of the trial functions which is used at the diagonalization of the nuclear Hamiltonian.

The generator coordinate method (GCM) [8,9] is one of the methods beyond the MFA which have been applied successfully to studies of the collective nuclear motions. For instance, the GCM has been applied to investigate the breathing-mode giant monopole resonance within the framework of the relativistic mean-field theory in [10]. In it the constrained incompressibility and the excitation energy of isoscalar giant monopole states were obtained for finite nuclei with various sets of Lagrangian parameters. An extension of the method of Ref. [10] by using a more general ansatz for the generating functions of the GCM and by including the isovector giant monopole states has been done in [11]. The use of the Skyrme effective forces has simplified the study of the monopole, dipole and quadrupole isoscalar and isovector vibrations in light double magic nuclei [12,13]. An approach to the GCM using square-well and harmonic-oscillator construction potentials has been applied to calculate the energies of the ground and first monopole excited state, as well as the density and the nucleon momentum distributions in the ground state of ^{4}He, ^{16}O and ^{40}Ca nuclei [14,15]. In [16] the occupation numbers, the depletion of the Fermi sea and the natural orbitals (NO) which diagonalize the ground state one-body density matrix (ODM) have been calculated. The NO related to the ground state and the single-particle potentials corresponding to them have been studied in detail in [17]. In [2,18] the two-nucleon center-of-mass and relative motion momentum distributions of $n-p$ pairs in the ^{4}He, ^{16}O and ^{40}Ca nuclei have been calculated. The existence of high-momentum components in the one-nucleon and two-nucleon momentum distributions in the case of the square-well construction potential with infinite walls within the GCM has been obtained. The studies of the energies, the nucleon momentum and density distributions in ^{4}He and ^{16}O nuclei have been extended by means of a two generator coordinate scheme in [19].

In the last years giant resonances with various multipolarities different from the well-known dipole resonance have been discovered. Among these collective excitations the monopole excitations take a particular place. The isoscalar giant monopole resonances or the so-called breathing vibrational states (with $I^\pi = 0^+$ at energies of approximately 13 to 20 MeV) have been well established experimentally (e.g. [20–27]) and have been considered to be compressional nuclear vibrations. Their study concerns the important problem of the compressibility of finite nuclei and nuclear matter (e.g. [28–33]). The description of such states is related mainly to general characteristics of the nuclei and weakly to the peculiarities of nuclear structure. Recently, in a series of articles Bishop et al.(see [34] and references therein) applied the translationally invariant cluster (TIC) method to light nuclei, in particular to the ^{4}He nucleus. The basic properties, such as the energies and the density distributions of the ground and first excited breathing mode state in ^{4}He have been considered.

The ^{4}He nucleus has a well-established spectrum of excited states. Calculations for the monopole oscillations of helium which practically involve the whole nuclear volume have been performed on the base of the nonlinear time-dependent Hartree-Fock (TDHF) approximation [35]. Its small amplitude limit, namely the random phase approximation (RPA), has been used extensively to describe nuclear collective motion [36]. The TDHF method [37] and the relativistic RPA [38] have been recently used to extend the study of isoscalar monopole modes in finite nuclei up to ^{208}Pb. It has been found that some effective Lagrangians can describe ground states and giant resonances as well, and in particular, they can predict correctly breathing mode energies in medium and heavy nuclei. In general, it has been pointed out that when going from heavy to lighter systems the trend is that the collectivity becomes weaker. This fact poses the question about the role of different kinds of nucleon-nucleon correlations corresponding to single-particle and collective motion modes and, therefore, the investigations on the correlation effects became an important task in the nuclear theory.

The aim of the present work is to study the main characteristics of the ground and, in particular, of the first excited monopole state in the ^{4}He, ^{16}O and ^{40}Ca nuclei within the GCM using Skyrme-type effective forces. It concerns the energies, the density distributions and radii, the nucleon momentum distributions, the natural orbitals and occupation numbers, as well as the pair center-of-mass and relative density and momentum distributions. As known, the natural orbital representation (NOR) [39] gives a model-independent effective single-particle picture for the correlated states. We emphasize that in our work this is done also for the first excited monopole state in the nuclei considered on the basis of the ODM calculated for this state. It is known that the results of the GCM calculations depend on the type of the construction potential used to define the generating function in the method. In the present work we use three construction potentials, namely the harmonic oscillator ((HO) where the oscillator parameter is a generator coordinate), the square-well with infinite walls ((SW) where the radius of the well is a generator coordinate) and Woods-Saxon ((WS1) where the diffuseness of the Woods-Saxon well is a generator coordinate and (WS2) where the radial parameter of Woods-Saxon well is a generator coordinate). The values of the radial parameter in the WS1 case and the diffuseness parameter in the WS2 case are taken from [40]. In our opinion, the calculations performed in this work can give an essential information about beyond MFA effects (accounted for in the considered approach to the GCM) on the mentioned characteristics. The results are compared with the available empirical data and with the calculations of other theoretical methods.

The basic relations of the GCM are given in Section 2. The results of the calculations and the discussion are presented in Section 3. The conclusions from the work are given in Section 4.

II. BASIC RELATIONS IN GCM

In the case of one real generator coordinate x the trial many-body wave function in the GCM is written as a linear combination [9]:

$$\Psi(\mathbf{r}_i) = \int_0^\infty f(x)\Phi(\{\mathbf{r}_i\}, x)dx\,, \quad i = 1..A\,, \tag{1}$$

where $\Phi(\{\mathbf{r}_i\}, x)$ is the generating function, $f(x)$ is the generator or weight function and A is the mass number of the nucleus.

The application of the Ritz variational principle $\delta E = 0$ leads to the Hill-Wheeler integral equation for the weight function:

$$\int_0^\infty [\mathcal{H}(x, x') - EI(x, x')]f(x')dx' = 0\,, \tag{2}$$

where

$$\mathcal{H}(x, x') =< \Phi(\{\mathbf{r}_i\}\, x)|\hat{H}|\Phi(\{\mathbf{r}_i\}\, x') >, \tag{3}$$

and

$$I(x, x') =< \Phi(\{\mathbf{r}_i\}\, x)|\Phi(\{\mathbf{r}_i\}\, x') > \tag{4}$$

are the energy and overlap kernels, respectively, and $\hat{H}$ is the Hamiltonian of the system.

If the generating function $\Phi(\{\mathbf{r}_i\}\, x)$ for a $N = Z$ nucleus is a Slater determinant built up from single-particle wave functions $\varphi_\lambda(\mathbf{r}, \mathbf{x})$ corresponding to a given construction potential then the energy kernel (3) has the form [41]:

$$\mathcal{H}(x, x') =< \Phi(\{\mathbf{r}_i\}\, x)|\Phi(\{\mathbf{r}_i\}\, x') > \int H(x, x', \mathbf{r})d\mathbf{r}\,. \tag{5}$$

In the case of the Skyrme-like forces (for nucleus with $Z = N$ and without Coulomb and spin-orbital interaction) $H(x, x', \mathbf{r})$ is given by:

$$H(x, x', \mathbf{r}) = \frac{\hbar^2}{2m}T + \frac{3}{8}t_0\rho^2 + \frac{1}{16}(3t_1 + 5t_2)(\rho T + \mathbf{j}^2) + \frac{1}{64}(9t_1 - 5t_2)(\nabla\rho)^2 + \frac{1}{16}t_3\rho^{2+\sigma}\,, \tag{6}$$

where $t_0, t_1, t_2, t_3, \sigma$ are the Skyrme-force parameters. The density ρ, the kinetic energy T and the current density $\mathbf{j}$ are defined by:

$$\rho(x, x', \mathbf{r}) = 4\sum_{\lambda,\mu=1}^{A/4}(N^{-1})_{\mu\lambda}\varphi^*_\lambda(\mathbf{r}, x)\varphi_\mu(\mathbf{r}, x')\,, \tag{7}$$

$$T(x, x', \mathbf{r}) = 4\sum_{\lambda,\mu=1}^{A/4}(N^{-1})_{\mu\lambda}\nabla\varphi^*_\lambda(\mathbf{r}, x)\cdot\nabla\varphi_\mu(\mathbf{r}, x')\,, \tag{8}$$

$$\mathbf{j}(x, x', \mathbf{r}) = 2\sum_{\lambda,\mu=1}^{A/4}(N^{-1})_{\mu\lambda}\{\varphi^*_\lambda(\mathbf{r}, x)\nabla\varphi_\mu(\mathbf{r}, x') - [\nabla\varphi^*_\lambda(\mathbf{r}, x)]\varphi_\mu(\mathbf{r}, x')\}\,, \tag{9}$$

where

$$N_{\lambda\mu}(x,x') = \int \varphi^*_\lambda(\mathbf{r},x)\varphi_\mu(\mathbf{r},x')d\mathbf{r}\,. \tag{10}$$

The overlap kernel (4) is given by:

$$I(x,x') = [det(N_{\lambda\mu})]^4\,. \tag{11}$$

Solving the Hill-Wheeler equation(2) one can obtain the solutions $f_0, f_1, ...$ for the weight functions which correspond to the eigenvalues of the energy $E_0, E_1....$

The one-body density matrix $\rho_i(\mathbf{r},\mathbf{r}')$ of the ground ($i=0$) and the first excited monopole ($i=1$) states in this GCM scheme has the form:

$$\rho_i(\mathbf{r},\mathbf{r}') = \int\!\!\int f_i(x)f_i(x')I(x,x')\rho(x,x',\mathbf{r},\mathbf{r}')dxdx'\,,\quad i=0,1\,, \tag{12}$$

where

$$\rho(x,x',\mathbf{r},\mathbf{r}') = 4\sum_{\lambda,\mu=1}^{A/4}(N^{-1})_{\mu\lambda}\varphi^*_\lambda(\mathbf{r},x)\varphi_\mu(\mathbf{r}',x')\,. \tag{13}$$

It follows from (12) that the nucleon density distribution $\rho_i(\mathbf{r})$ and the nucleon momentum distribution $n_i(\mathbf{k})$ of the ground and the first excited monopole states can be expressed as:

$$\rho_i(\mathbf{r}) = \int\!\!\int f_i(x)f_i(x')I(x,x')\rho(x,x',\mathbf{r})dxdx'\,,\quad i=0,1 \tag{14}$$

and

$$n_i(\mathbf{k}) = \int\!\!\int f_i(x)f_i(x')I(x,x')\rho(x,x',\mathbf{k})dxdx'\,,\quad i=0,1\,, \tag{15}$$

where

$$\rho(x,x',\mathbf{r}) = \rho(x,x',\mathbf{r},\mathbf{r}'=\mathbf{r})\,, \tag{16}$$

$$\rho(x,x',\mathbf{k}) = 4\sum_{\lambda,\mu=1}^{A/4}(N^{-1})_{\mu\lambda}\tilde{\varphi}^*_\lambda(\mathbf{k},x)\tilde{\varphi}_\mu(\mathbf{k},x') \tag{17}$$

and $\tilde{\varphi}(\mathbf{k},x)$ is the Fourier transform of $\varphi(\mathbf{r},x)$.

The rms radii can be calculated using the expression:

$$r^{(i)}_{rms} = \sqrt{\frac{\int r^4\rho_i(r)dr}{\int r^2\rho_i(r)dr}}\,,\quad i=0,1\,. \tag{18}$$

As shown e.g. in [1,42] the attractive properties of the single-particle description can be preserved in the correlation methods using the natural orbital representation [39]. In it the one-body density matrix has the simple form:

$$\rho_i(\mathbf{r},\mathbf{r}') = \sum_\alpha n^{(i)}_\alpha \psi^{(i)*}_\alpha(\mathbf{r})\psi^{(i)}_\alpha(\mathbf{r}')\,,\quad i=0,1\,, \tag{19}$$

where the natural orbitals (NO) $\psi^{(i)}_\alpha(\mathbf{r})$ form a complete orthonormal set of single-particle wave functions which diagonalize the density matrix $\rho_i(\mathbf{r},\mathbf{r}')$ for the ground and the first excited monopole states. The natural occupation numbers (ON) $n^{(i)}_\alpha$ for the state α satisfy the conditions:

$$0\le n_\alpha^{(i)}\le 1, \qquad \sum_\alpha n_\alpha^{(i)} = A\,. \tag{20}$$

It is seen from (19) that the natural orbitals and the occupation numbers can be found solving the equation:

$$\int \rho_i(\mathbf{r},\mathbf{r}')\psi_\alpha^{(i)}(\mathbf{r}')d\mathbf{r}' = n_\alpha^{(i)}\psi_\alpha^{(i)}(\mathbf{r})\,, \quad i=0,1\,. \tag{21}$$

For nuclei with total spin $J=0$ the one-body density matrix can be diagonalized in the $\{l\,j\,m\}$ subspace (l,j,m being the quantum numbers corresponding to the angular momentum, total momentum and its projection). In the case of nuclei with spherical symmetry the natural orbitals have the form:

$$\psi_{nlm}^{(i)}(\mathbf{r}) = R_{nl}^{(i)}(r)Y_{lm}(\theta,\varphi) = \frac{u_{nl}^{(i)}(r)}{r}Y_{lm}(\theta,\varphi)\,, \quad i=0,1\,, \tag{22}$$

where $R_{nl}^{(i)}(r)$ is the radial part of the NO's and $Y_{lm}(\theta,\varphi)$ is the spherical function. The substitution of $\psi_{nlm}^{(i)}(\mathbf{r})$ from (22) and $\rho_i(\mathbf{r},\mathbf{r}')$ from (12) in equation (21) and the integration over the angular variables give the following equation for the radial part $u_{nl}^{(i)}(r)$ of the NO's and the occupation numbers $n_{nl}^{(i)}$:

$$\int_0^\infty K_l^{(i)}(\mathbf{r},\mathbf{r}')u_{nl}^{(i)}(r')dr' = n_{nl}^{(i)}u_{nl}^{(i)}(r)\,, \quad i=0,1\,, \tag{23}$$

where

$$K_l^{(i)}(\mathbf{r},\mathbf{r}') = rr'\int\!\!\int f_i(x)f_i(x')I(x,x')\sum_{n,n'}(N^{-1})_{nl,n'l}\mathcal{R}^*_{n'l}(r,x)\mathcal{R}_{nl}(r',x')dxdx'\,, \quad i=0,1\,. \tag{24}$$

The summation in (24) is performed over all single-particle wave functions with given l forming the Slater determinant of the generating function and $\mathcal{R}_{nl}(r,x)$ are the radial parts of these functions.

The nucleon density distribution $\rho_i(r)$ and the nucleon momentum distribution $n_i(k)$ for nuclei with $J=0$ can be written in the following form in the NOR:

$$\rho_i(r) = \frac{1}{4\pi}\sum_l 2(2l+1)\sum_n n_{nl}^{(i)}|R_{nl}^{(i)}(r)|^2\,, \quad i=0,1\,, \tag{25}$$

$$n_i(k) = \frac{1}{4\pi}\sum_l 2(2l+1)\sum_n n_{nl}^{(i)}|\tilde{R}_{nl}^{(i)}(k)|^2\,, \quad i=0,1\,, \tag{26}$$

where

$$\tilde{R}_{nl}^{(i)}(k) = (\frac{2}{\pi})^{1/2}(-i)^l\int_0^\infty r^2 j_l(kr)R_{nl}^{(i)}(r)dr\,, \quad i=0,1 \tag{27}$$

is the radial part of the NO in the momentum space and $j_l(kr)$ are spherical Bessel functions of order l.

The depletion of the Fermi sea can be defined by the expression:

$$\mathcal{D}^{(i)} = \frac{4}{A}\sum_{j,\alpha\in\{F\}}(2j+1)(1-n_\alpha^{(i)})\,, \quad i=0,1\,, \tag{28}$$

where $\{F\}$ refers to the Fermi sea.

The rms radius of the NO $\psi_\alpha^{(i)}(\mathbf{r})$ is given by the expression:

$$< r_\alpha^{(i)} >= \sqrt{\frac{\int r^2|\psi_\alpha^{(i)}(\mathbf{r})|^2 d\mathbf{r}}{\int |\psi_\alpha^{(i)}(\mathbf{r})|^2 d\mathbf{r}}}\,, \quad i=0,1\,. \tag{29}$$

The two-body density matrix $\rho^{(2)}(\xi_1,\xi_2;\xi_1',\xi_2')$ in the GCM has the form:

$$\rho^{(2)}(\xi_1,\xi_2;\xi_1',\xi_2') = \int dx f^*(x) \int dx' f(x')\rho^{(2)}(x,x';\xi_1,\xi_2;\xi_1',\xi_2') \ , \tag{30}$$

where the coordinate ξ includes the spatial coordinate $\mathbf{r}$, as well as the spin (s) and isospin (τ) variables. If the generating wave function is a Slater determinant constructed from a complete set of one-particle wave functions $\varphi_i(x,\xi)$ the matrix $\rho^{(2)}(x,x';\xi_1,\xi_2;\xi_1',\xi_2')$ can be expressed as [39]:

$$\rho^{(2)}(x,x';\xi_1,\xi_2;\xi_1',\xi_2') = \frac{I(x,x')}{2} \det \begin{pmatrix} \rho^{(2)}(x,x';\xi_1,\xi_1') & \rho^{(2)}(x,x';\xi_1,\xi_2') \\ \rho^{(2)}(x,x';\xi_2,\xi_1') & \rho^{(2)}(x,x';\xi_2,\xi_2') \end{pmatrix} \ , \tag{31}$$

where

$$\rho^{(2)}(x,x';\xi,\xi') = \sum_{k,l=1}^{A} \left(N^{-1}\right)_{lk} \varphi_k^*(x,\xi)\varphi_l(x',\xi') \ , \tag{32}$$

$\left(N^{-1}\right)_{lk}$ is the inverse matrix of:

$$N_{kl}(x,x') = \sum_{s,\tau} \int d\mathbf{r}\varphi_k^*(x,\xi)\varphi_l(x',\xi) \ , \tag{33}$$

and

$$I(x,x') = \det\left(N_{kl}\right) \ . \tag{34}$$

The two-particle emission experiments require some knowledge of physical quantities associated with the TDM. For example, using the two-body density matrix $\rho^{(2)}$ in coordinate space, Eq.(30), one can define the pair center-of-mass local density distribution:

$$\rho^{(2)}(\mathbf{R}) = \int \rho^{(2)}(\mathbf{R}+\mathbf{s}/2, \mathbf{R}-\mathbf{s}/2) d\mathbf{s} \tag{35}$$

and the pair relative local density distribution:

$$\rho^{(2)}(\mathbf{s}) = \int \rho^{(2)}(\mathbf{R}+\mathbf{s}/2, \mathbf{R}-\mathbf{s}/2) d\mathbf{R} \,. \tag{36}$$

In momentum space the associated pair center-of-mass and relative momentum distributions can be defined:

$$n^{(2)}(\mathbf{K}) = \int n^{(2)}(\mathbf{K}/2+\mathbf{k}, \mathbf{K}/2-\mathbf{k}) d\mathbf{k} \,, \tag{37}$$

$$n^{(2)}(\mathbf{k}) = \int n^{(2)}(\mathbf{K}/2+\mathbf{k}, \mathbf{K}/2-\mathbf{k}) d\mathbf{K} \,. \tag{38}$$

The physical meaning of $\rho^{(2)}(\mathbf{s})$ and $n^{(2)}(\mathbf{k})$ is the probability to find two particles displaced of a certain relative distance $\mathbf{s} = \mathbf{r}_1 - \mathbf{r}_2$ or moving with relative momentum $\mathbf{k} = (\mathbf{k}_1 - \mathbf{k}_2)/2$, respectively, while $\rho^{(2)}(\mathbf{R})$ and $n^{(2)}(\mathbf{K})$ represent the probability to find a pair of particles with center-of-mass coordinate $\mathbf{R} = (\mathbf{r}_1 + \mathbf{r}_2)/2$ or center-of-mass momentum $\mathbf{K} = \mathbf{k}_1 + \mathbf{k}_2$.

III. RESULTS AND DISCUSSION

A. The ground and first excited collective state energies

The Hill-Wheeler equation (2) is solved using a discretization procedure similar to that of Refs. [12,13]. The values of the Skyrme-force parameters in (6) in the case of square-well construction potential are the same as in [15]. They are determined to give an optimal fit to the binding energies of ^{4}He, ^{16}O and ^{40}Ca obtained from the Hill-Wheeler equation (2). The parameter set values $t_0 = -2765, t_1 = 383.94, t_2 = -38.04, t_3 = 15865, \sigma = 1/6$ lead to the energies of the ground E_0 and the first monopole excited E_1 states (without the Coulomb energy) shown in Table I. In the case of the harmonic-oscillator and Woods-Saxon construction potentials SkM* parameter set values ($t_0 = -2645, t_1 = 410, t_2 = -135, t_3 = 15595, \sigma = 1/6$) [43] giving realistic binding energies are used. It can be seen from Table I that the energies obtained with WS1 are close to that obtained with HO, while the energies corresponding to WS2 are closer to that calculated with SW construction potential.

The values of the excitation energies $\Delta E = E_1 - E_0$ of the first monopole state ($I^\pi = 0^+$) calculated within the GCM are given and compared with other calculations and some experimental data in Table II. It is seen that the GCM results with HO construction potential and in the WS1 case are in good agreement with the result of Brink and Nash [44] for ^{16}O nucleus and they are closer to the experimental values than the GCM results with the SW construction potential. The energy of the first excited 0^+ in ^{4}He obtained in the present work is compared in Table II with the recent refined calculations of Bishop et al [34] within the TIC method as well as with the results of the coupled rearrangement of the channels method [45].

B. The one-body density matrix $\rho(\mathbf{r}, \mathbf{r}')$ of the ground and first excited monopole states

1. The nucleon density distribution $\rho(\mathbf{r})$

The one-body distribution function corresponding to the density distribution $\rho_i(\mathbf{r})$ from (14) is given by the expression:

$$g_i(r) = 4\pi r^2 \rho_i(r)\,, \quad i = 0, 1\,. \tag{39}$$

The function $g_i(r)$ of the ground (i=0) and the first excited monopole (i=1) states of ^{4}He calculated in the GCM are compared in Figure 1 with those obtained in the TIC method. It can be seen that there is a large difference in the behaviour of the function $g(r)$ for both states. This is due to the strong increase of the size of the nucleus, as is shown in Table III: the rms radius increases from 1.89 fm for the ground state to 3.00 fm for the first excited monopole state in the case of the HO, from 1.77 fm to 2.86 fm in the case of the SW and from 1.85 fm to 3.29 fm when using WS2. The significantly larger values of rms radii for the first excited state in ^4He nucleus in respect to their ground state values support the breathing-mode interpretation. At the same time, the nature of the first excited monopole state in ^4He is not still well understood. An attempt to solve this problem is made in Ref. [46] where it is concluded that the $i = 1$ state is dominated by the $^3H + p$ configuration. The rms radii of the ground and of the first excited monopole states in ^{16}O and ^{40}Ca are also presented in Table III. We note that the rms radii of the ground state in these nuclei obtained with Woods-Saxon construction potential are very close to the experimental values.

For the first excited monopole state the one-body distribution function $g_1(r)$ calculated within the GCM using the WS2 potential and that one calculated within the TIC method are in good agreement. In contrast with this state, for a ground state both methods yield functions $g_0(r)$ which differ significantly. This is due to the spurious centre-of-mass motion correction for ^{4}He which is accounted for in the TIC method [34]. At the same time effect doesn't influence substantially the first excited monopole-state density.

The nucleon density distributions of ^{16}O and ^{40}Ca of the ground ρ_0 and the first excited monopole ρ_1 states obtained within the GCM are presented in Figures 2 and 3, respectively. For the first excited monopole state the density distribution $\rho_1(r)$ decreases in the central region of both nuclei and increases for large r. This behaviour corresponds to the increase of the rms radius in the first excited state. It can be seen also that the difference in the rms radii $\Delta r_{rms} = r_{rms}^{(1)} - r_{rms}^{(0)}$ decreases with the increase of the mass number.

2. The nucleon momentum distribution $n(\mathbf{k})$

The nucleon momentum distribution $n(\mathbf{k})$ is one of the nuclear quantities which are sensitive to various types of nucleon-nucleon correlations. The momentum distributions for the ground and first excited monopole states of ^{16}O have been calculated in the GCM using Eqs.(15) and (17) and are shown in Figure 4. As can be seen there is no essential difference between the behaviour of the $n(\mathbf{k})$ in the ground and in the first excited monopole states.

It is seen from Figure 4 that the nucleon momentum distribution $n(\mathbf{k})$ obtained in the GCM depends on the construction potentials considered. The use of SW potential leads to an existence of high-momentum tail of $n(\mathbf{k})$ which is not the case when the HO and WS potentials are used. Here we would like to note that:

(i) the single-particle wave functions corresponding to the SW potential contain themselves high-momentum components due to the particular form of the potential and they are reflected in the GCM result,

(ii) the lack of substantial high-momentum tail in $n(\mathbf{k})$ when using HO and WS construction potential leads to the conclusion that the nucleon-nucleon correlations included in the GCM approach are not of short-range type. An additional study of the correlations accounted for in the GCM concerns some two-body characteristics and we will discuss the results for them in subsection C.

3. The natural orbitals and occupation numbers

The natural orbitals and occupation numbers have been calculated using Eqs.(21)-(24). A discretization procedure with respect to both r and r' has been applied solving Eq.(23) and the resulting matrix eigenvalue problem has been solved numerically. The natural orbitals obtained in the coordinate space are plotted in Figure 5 for the ^{16}O nucleus. The corresponding rms radii and the natural occupation numbers of ^{4}He, ^{16}O and ^{40}Ca are shown in Tables 4 and 5, respectively.

One can see from Table IV and from the shape of the NO's given in Figure 5 that the rms radii of the natural hole-states increase from the ground state to the first excited state. The occupation numbers of the natural hole-states decrease in the first excited monopole state, while those corresponding to the natural particle-states increase (see Table V). As can be seen from the same Table V, the depletion of the Fermi sea increases in the first excited state. This is strongly expressed for the ^{4}He nucleus. The calculated depletion decreases with the increase of the mass number.

C. The pair center-of-mass and relative density and momentum distributions

The pair center-of-mass and relative density and momentum distributions Eqs.(35)-(38) are calculated by using of HO and SW potentials and are given in Figure 6 for the ground state of ^{16}O nucleus. They are compared with the results obtained within the low-order approximation of the Jastrow correlation method (JCM) [48] where the short-range correlations are explicitely involved. As it is seen from Figure 6(a') the relative distributions $\rho^{(2)}(\mathbf{s})$ obtained in GCM and JCM have different behaviour in the region from 0 to 0.4 fm. This fact shows that the GCM doesn't take into account short-range but other kind of correlations which are obviously related with the collective motion of the nucleons. The curves of $n^{(2)}(\mathbf{K})$ calculated for both potentials decrease rapidly down at K>1fm^{-1} while the result obtained within the JCM shows a high-momentum tail.

IV. CONCLUSION

In the present work the characteristics of the ground and the first excited monopole states of the three nuclei ^{4}He, ^{16}O and ^{40}Ca are studied within the GCM using different construction potentials. Though the results are sensitive to the type of the construction potentials used, some general conclusions can be summarized as follows

(i) There is an increase of the rms radius in the first excited monopole state as a consequence of the increase of the density distribution for large r.

(ii) There is not an essential difference between the behaviour of the nucleon momentum distribution in the ground and in the first excited monopole state.

(iii) The use of the natural orbital representation makes it possible to study the effective single-particle picture not only of the ground, but also of the first excited monopole state. It is established that the depletion of the Fermi sea increases considerably in the first excited monopole state. This is strongly expressed in the case of ^{4}He. The calculated depletion decreases with the increase of the mass number.

(iv) The study of the natural orbitals in the ground and the first excited monopole state shows that there are not substantial changes in their forms for a given nl-state when they are calculated for the ground and the first excited monopole state. The rms radii of the hole-state natural orbitals are larger in the case of the first excited monopole state in comparison with those for the ground state.

(v) The results on the one- and two-body density and momentum distributions, occupation probabilities and natural orbitals obtained within the GCM using various construction potentials show that the nucleon-nucleon correlations accounted in the approach are different from the short-range ones but are rather related to the collective motion of the nucleons. It turns out that the latter are also important in calculations of one- and two-body overlap functions which are necessary in the calculations of the cross-sections of one- and two-nucleon removal reactions. The work on the applications of the GCM overlap functions for the description of cross-section of (p,d), $(e,e'p)$ and (γ,p) reactions is in progress.

V. ACKNOWLEDGMENTS

This work was partly supported by the Bulgarian National Science Foundation under the Contract No.Φ-809.

---

[1] A.N. Antonov, P.E. Hodgson, I.Zh. Petkov, *Nucleon Momentum and Density Distributions in Nuclei* (Clarendon Press, Oxford 1988)

[2] A.N. Antonov, P.E. Hodgson, I.Zh. Petkov, *Nucleon Correlations in Nuclei* (Springer-Verlag, Berlin-Heidelberg-New York, 1993)

[3] O. Bohigas, S. Stringari, Phys. Lett. **95B**, 9 (1980)

[4] M. Jaminon, C. Mahaux, H. Ngô, Phys. Lett. B **158**, 103 (1985)

[5] B. Frois, C. Papanicolas, Ann. Rev. Nucl. Part. Sci. **37**, 133 (1987)

[6] L. Lapikás, in *Proceedings of 6th International Conference on Nuclear Reaction Mechanisms, Varena, 1991*, edited by E. Gadioli (Ricerca Scintifica ed Educazione Permanente, Milano, 1991), p. 610

[7] L. Lapikás, EMIN 92-06, 1992 (Amsterdam)

[8] D.L. Hill, J.A. Wheeler, Phys. Rev. **89**, 1102 (1953)

[9] J.J. Griffin, J.A. Wheeler, Phys. Rev. **108**, 311 (1957)

[10] M.V. Stoitsov, P. Ring, M.M. Sharma, Phys. Rev. C **50**, 1445 (1994)

[11] D. Vretenar, G.A. Lalazissis, R. Behnsch, W. Pöschl, P. Ring, nucl-th/9612042, 1996 (Los Alamos)

[12] H. Flocard, D. Vautherin, Phys. Lett. B **55**, 259 (1975)

[13] H. Flocard, D. Vautherin, Nucl. Phys. A **264**, 197 (1976)

[14] A.N. Antonov, Chr.V. Christov, I.Zh. Petkov, Nuovo Cimento A **91**, 119 (1986)

[15] A.N. Antonov, I.S. Bonev, Chr.V. Christov, I.Zh. Petkov, Nuovo Cimento A **100**, 779 (1988)

[16] A.N. Antonov, I.S. Bonev, Chr.V. Christov, E.N. Nikolov, I.Zh. Petkov, Nuovo Cimento A **103**, 1287 (1990)

[17] A.N. Antonov, D.N. Kadrev, P.E. Hodgson, Phys. Rev. C **50**, 164 (1994)

[18] A.N. Antonov, I.S. Bonev, I.Zh. Petkov, JINR Rapid Communications, No 1[40]-90, 35 (1990); Bulg. J. Phys. **18**, 169 (1991)

[19] A.N. Antonov, M.V. Stoitsov, L.P. Marinova, M.E. Grypeos, G.A. Lalazissis, K.N. Ypsilantis, Phys. Rev. C **50**, 1936 (1994)

[20] D.H. Youngblood, P. Bogucki, J.D. Bronson, U. Gard, Y.W. Lui, C.M. Rosza, Phys. Rev. C **23**, 1997 (1981)

[21] J. Speth, A. van der Woude, Rep. Progr. Phys **44**, 719 (1981)

[22] N.A. Voinova-Eliseeva, I.A. Mitropolsky, LINP 1104, 1985 (Leningrad)

[23] Y.W. Lui, J.D. Bronson, D.H. Youngblood, Y. Toba, U. Garg, Phys. Rev. C **31**, 1643 (1985)

[24] H.Y. Lu, S. Brandenburg, R. de Leo, M.N. Harakeh, T.D. Poelhekken, A. van der Woude, Phys. Rev. C **33**, 1166 (1986)

[25] S. Brandenburg, W.T.A. Borghols, A.G. Drentje, L.P. Ekström , M.N. Harakeh, A. van der Woude, A. Håkansson, L. Nilsson, N. Olsson, M. Pignanelli, R. de Leo, Nucl. Phys. A **466**, 29 (1987)

[26] M.M. Sharma, W.T.A. Borghols, S. Brandenburg, S. Crona, A. van der Woude, M.N. Harakeh, Phys. Rev. C **38**, 2562 (1988)

[27] W.T.A. Borghols, S. Brandenburg, J.H. Meier, J.M. Schippers, M.M. Sharma, A. van der Woude, M.N. Harakeh, A. Lindholm, L. Nilsson, S. Orona, A. Håkansson, L.P. Ekström, N. Olsson, R. de Leo, Nucl. Phys. A **504**, 231 (1989)

[28] A.N. Antonov, V.A. Nikolaev, I.Zh. Petkov, Bulg. J. Phys **18**, 107 (1991)

[29] K.A. Brueckner, M.J. Giannoni, R.J. Lombard, Phys. Lett. B **31**, 97 (1970)

[30] V.R. Pandharipande, Phys. Lett. B **31**, 635 (1970)

[31] J. Treiner, H. Krivine, O. Bohigas, J. Martorell, Nucl. Phys. A **371**, 253 (1981)

[32] N.A. Voinova-Eliseeva, I.A. Mitropolsky, LINP 1095, 1985 (Leningrad)

[33] M.M. Sharma, W. Stocker, P. Gleissl, M. Brack, Nucl. Phys. A **504**, 337 (1989)

[34] R.F. Bishop, E. Buendia, M.F. Flynn, R. Guardiola, J. Phys. G **19**, 1163 (1993)

[35] J.S. Wu, K.C. Wong, M.R. Strayer, M. Baranger, Phys. Rev. C **56**, 857 (1997)

[36] G. Colò, N. Van Giai, P. Bortignon, A. Bracco, R. Broglia, Fizika **22**, 267 (1990); Phys. Lett. B **276**, 279 (1992)

[37] J.S. Wu, M.R. Strayer, M. Baranger, Phys. Rev. C **60**, 044302 (1999)

[38] Z. Ma, N. Van Giai, H. Toki, M. L'Huillier, Phys. Rev. C **55**, 2385 (1997)

[39] P.-O. Löwdin, Phys. Rev. **97**, 1474 (1955)

[40] H.P. Blok and J.H. Heisenberg, in *Computational Nuclear Physics 1, Nuclear Structure*, Edited by K. Langanke, J.A. Maruhn, S.E. Koonin (Springer-Verlag, Berlin, 1991), p. 190.

[41] D.M. Brink,in *Proc. S I F, Course XXXVI*, edited by C. Bloch (Academic Press, New York, 1966), p. 247

[42] A.N. Antonov, Chr.V. Christov, E.N. Nikolov, I.Zh. Petkov, P.E. Hodgson, Nuovo Cimento A **102**, 1701 (1989)

[43] J. Bartel, P. Quentin, M. Brack, C. Guet, H.B. Håkansson, Nucl. Phys. A**386**, 79 (1982)

[44] D.M. Brink, G.F. Nash, Nucl. Phys. **40**, 608 (1963)

[45] H. Kameyama, M. Kamimura, Y. Fukushima, Phys. Rev. C **40**, 974 (1989)

[46] A. Csóto, G.M. Hale, Phys. Rev. C **55**, 2366 (1997)

[47] J. Cerny, R.H. Pehl, G.T. Garvey, Phys. Lett. **12**, 234 (1964)

[48] S.S. Dimitrova, D.N. Kadrev, A.N. Antonov, M.V. Stoitsov, nucl-th/9904071; Condensed Matter Theories, v.15, Nova (in print)

Figure Captions

Figure 1. One-body distribution function (Eq.(39)) $g(r)$ of ^{4}He calculated within the GCM using harmonic-oscillator (a), square-well (b) and Woods-Saxon (c) potentials and within the TIC method [34]. The normalization is: $\int g_i(r)dr = 1 \;\; (i = 0, 1)$.

Figure 2. Nucleon density distributions of the ground (ρ_0) and the first excited monopole (ρ_1) states of ^{16}O calculated within the GCM using harmonic-oscillator (a), square-well (b) and Woods-Saxon (c) potentials. The normalization is: $\int \rho_i(\mathbf{r})d\mathbf{r} = 16 \;\; (i = 0, 1)$.

Figure 3. The same as in Figure 2 but for ^{40}Ca.

Figure 4. Nucleon momentum distributions of the ground (n_0) and the first excited monopole (n_1) states of ^{16}O calculated within the GCM using harmonic-oscillator (a), square-well (b) and Woods-Saxon (c) potentials. The normalization is: $\int n_i(k)k^2dk = 16 \;\; (i = 0, 1)$.

Figure 5. Natural orbitals for the 1s-hole (a, a′, a′′), 1p-hole (b, b′, b′′) and 2s-particle (c, c′, c′′) states of the ground ($i = 0$) and of the first excited monopole ($i = 1$) states of ^{16}O in coordinate space calculated within the GCM using harmonic-oscillator, square-well and Woods-Saxon potentials, respectively.

Figure 6. The pair center-of-mass $\rho^{(2)}(\mathbf{R})$ (a) and relative $\rho^{(2)}(\mathbf{s})$ (a′) density distributions and the pair center-of-mass $n^{(2)}(\mathbf{K})$ (b) and relative $n^{(2)}(\mathbf{k})$ (b′) momentum distributions of the ground state of ^{16}O calculated within the GCM using harmonic-oscillator and square-well potentials. The results obtained within the Jastrow correlation method [48] are also given. The normalization is: $\int n^{(2)}(\mathbf{K})d\mathbf{K} = 1$, $\int n^{(2)}(\mathbf{k})d\mathbf{k} = 1$, $\int \rho^{(2)}(\mathbf{R})d\mathbf{R} = A*(A-1)/2$, $\int \rho^{(2)}(\mathbf{s})d\mathbf{s} = A*(A-1)/2$

TABLE I. Energies (in MeV) of the ground and the first excited monopole states in GCM with square-well, harmonic-oscillator and Woods-Saxon construction potentials (without the Coulomb energy).

Nuclei	Energies	GCM HO	GCM SW	GCM WS1	GCM WS2
^{4}He	E_0	-29.51	-37.10	-26.31	-28.03
	E_1	-8.06	-9.87	-5.38	-8.29
^{16}O	E_0	-139.96	-144.80	-137.99	-139.58
	E_1	-115.01	-111.66	-114.09	-112.50
^{40}Ca	E_0	-410.07	-404.23	-409.23	-411.40
	E_1	-387.58	-370.72	-386.13	-384.92

TABLE II. The excitation energies of 0^+ breathing states (in MeV).

	^{4}He	^{16}O	^{40}Ca
GCM(HO)	21.45	24.95	22.49
GCM(SW)	27.23	33.14	33.51
GCM(WS1)	20.93	23.90	23.10
GCM(WS2)	19.74	27.08	26.48
Ref. [2]		23.20	27.30
Ref. [44]		24	
Ref. [30]			18.3
Ref. [29] η=8		30.5	29.5
Ref. [29] η=12		30.0	26.5
Ref. [34]	24.96		
Ref. [45]	22.86		
Ref. [37]	26.49	29.49	
EXP		22.9 (T=2) [47]	20.0 (T=0) [22]

TABLE III. Rms radii (in fm) of the ground and the first excited monopole states (first and second row, respectively) in ^{4}He, ^{16}O and ^{40}Ca obtained with HO, SW, WS1 and WS2 construction potentials.

Nuclei	GCM HO	GCM SW	GCM WS1	GCM WS2
^{4}He	1.89	1.77	2.28	1.85
	3.00	2.86	3.43	3.29
^{16}O	2.67	2.63	2.70	2.71
	2.87	2.90	2.89	2.90
^{40}Ca	3.37	3.40	3.38	3.39
	3.45	3.52	3.48	3.51

TABLE IV. Rms radii (in fm) corresponding to the natural orbitals of the ground and the first excited monopole state calculated in the GCM with HO, SW, WS1 and WS2 construction potentials. The Fermi level is denoted by (*).

^{4}He-ground state					^{4}He-first excited monopole state				
state	HO	SW	WS1	WS2	state	HO	SW	WS1	WS2
3s	3.44	1.57	5.45	4.69	3s	3.40	4.92	2.68	2.91
2s	1.78	2.77	2.62	2.84	2s	2.80	2.37	3.03	4.21
1s*	1.88	1.76	2.26	1.84	1s*	3.03	2.91	3.44	3.11
^{16}O-ground state					^{16}O-first excited monopole state				
state	HO	SW	WS1	WS2	state	HO	SW	WS1	WS2
2p	3.32	3.65	3.82	4.89	2p	3.79	3.57	4.11	3.98
2s	2.97	3.59	2.68	4.44	2s	3.36	3.55	3.82	3.29
1p*	2.81	2.70	2.87	2.85	1p*	2.97	2.92	2.97	2.96
1s	2.18	2.35	2.13	2.21	1s	2.29	2.53	2.19	2.30
^{40}Ca-ground state					^{40}Ca-first excited monopole state				
state	HO	SW	WS1	WS2	state	HO	SW	WS1	WS2
3s	4.22	4.48	4.92	6.09	3s	4.57	4.41	5.03	3.68
2d	4.28	4.55	4.88	4.63	2d	4.58	4.51	5.00	3.66
2p	3.88	4.49	4.28	3.08	2p	4.14	4.46	4.86	3.73
2s*	3.62	3.56	3.98	3.85	2s*	3.71	3.65	4.02	3.82
1d	3.64	3.59	3.63	3.63	1d	3.70	3.67	3.71	3.73
1p	3.08	3.32	3.06	3.14	1p	3.13	3.39	3.09	3.27
1s	2.42	2.25	2.04	2.20	1s	2.40	2.29	2.13	2.46

TABLE V. Occupation numbers and total depletion $\mathcal{D}$ (Eq.(28)) of the ground and the first excited monopole state calculated in the GCM with HO, SW, WS1 and WS2 construction potentials. The Fermi level is denoted by (*).

	^{4}He-ground state					^{4}He-first excited monopole state			
state	HO	SW	WS1	WS2	state	HO	SW	WS1	WS2
3s	$< 10^{-3}$	0.002	$< 10^{-3}$	$< 10^{-3}$	3s	0.003	0.009	$< 10^{-3}$	$< 10^{-3}$
2s	0.005	0.014	0.024	0.006	2s	0.149	0.152	0.045	0.142
1s*	0.995	0.984	0.975	0.993	1s*	0.843	0.886	0.955	0.8576
$\mathcal{D}$	0.5%	1.6%	2.5%	0.7%	$\mathcal{D}$	15.7%	11.4%	4.5%	14.2%
	^{16}O-ground state					^{16}O-first excited monopole state			
state	HO	SW	WS1	WS2	state	HO	SW	WS1	WS2
2p	$< 10^{-3}$	0.013	$< 10^{-3}$	0.003	2p	0.067	0.095	0.08	0.07
2s	$< 10^{-3}$	0.008	$< 10^{-3}$	0.003	2s	0.040	0.057	0.02	0.07
1p*	0.999	0.986	1.000	0.999	1p*	0.930	0.903	0.933	0.926
1s	1.000	0.992	1.000	0.999	1s	0.956	0.942	0.990	0.955
$\mathcal{D}$	< 0.1%	1.2%	< 0.1%	< 0.1%	$\mathcal{D}$	6.4%	8.7%	5.3%	6.7%
	^{40}Ca-ground state					^{40}Ca-first excited monopole state			
state	HO	SW	WS1	WS2	state	HO	SW	WS1	WS2
3s	$< 10^{-3}$	0.014	$< 10^{-3}$	$< 10^{-3}$	3s	0.041	0.076	0.038	0.024
2d	$< 10^{-3}$	0.010	$< 10^{-3}$	$< 10^{-3}$	2d	0.029	0.055	0.036	0.024
2p	$< 10^{-3}$	0.007	$< 10^{-3}$	$< 10^{-3}$	2p	0.021	0.039	0.011	0.026
2s*	0.999	0.986	1.000	0.993	2s*	0.952	0.923	0.960	0.969
1d	0.999	0.990	1.000	0.993	1d	0.964	0.945	0.963	0.970
1p	0.999	0.993	1.000	0.993	1p	0.972	0.961	0.988	0.968
1s	1.000	1.000	1.000	0.994	1s	0.993	1.000	0.998	0.994
$\mathcal{D}$	< 0.1%	0.9%	< 0.1%	0.6%	$\mathcal{D}$	3.2%	4.7%	2.6%	2.8%

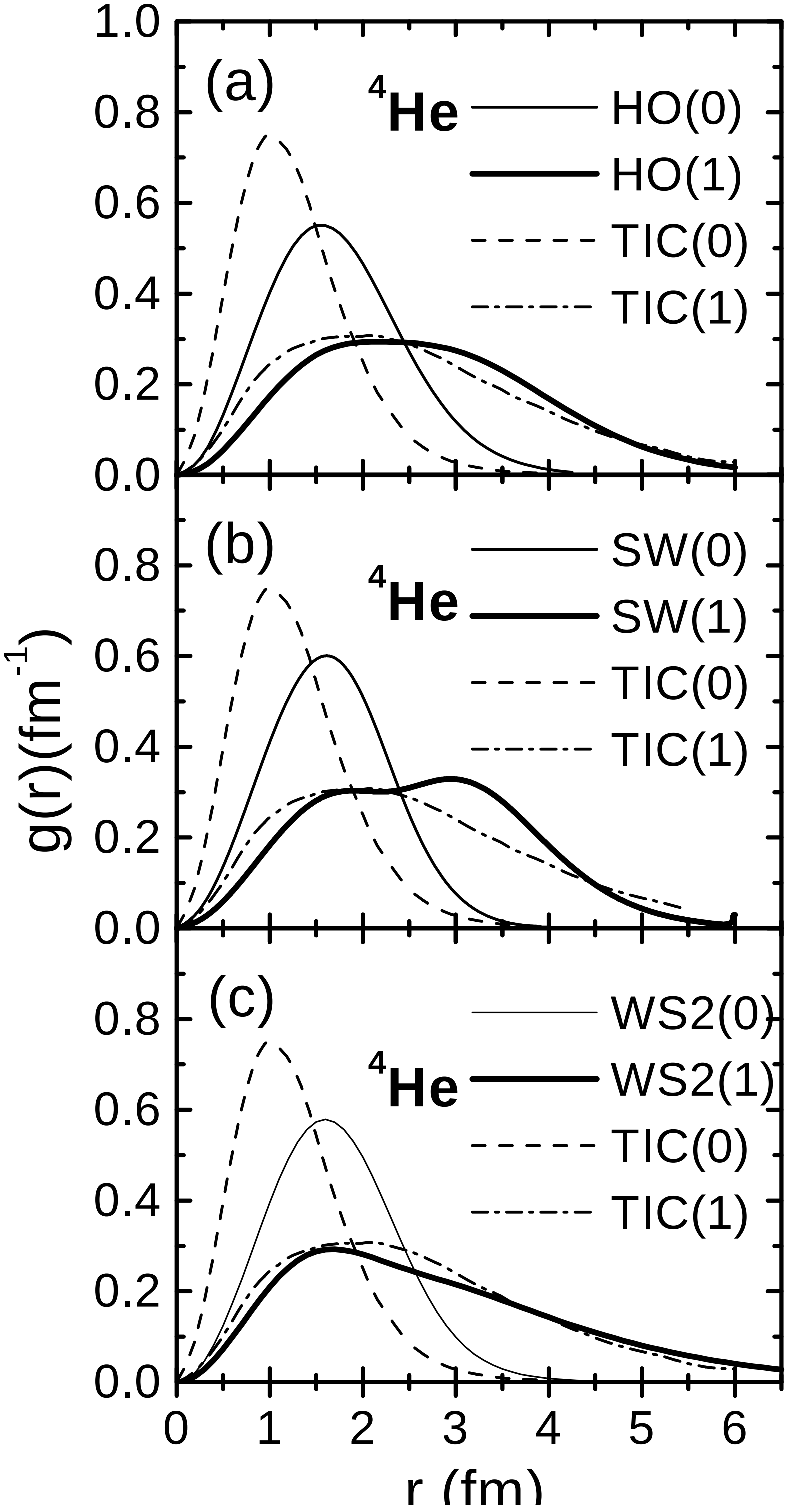

(a)
^{4}He
HO(0)
HO(1)
TIC(0)
TIC(1)
(b)
^{4}He
SW(0)
SW(1)
TIC(0)
TIC(1)
(c)
^{4}He
WS2(0)
WS2(1)
TIC(0)
TIC(1)
g(r)(fm^{-1})
r (fm)
1.0
0.8
0.6
0.4
0.2
0.0
0
1
2
3
4
5
6

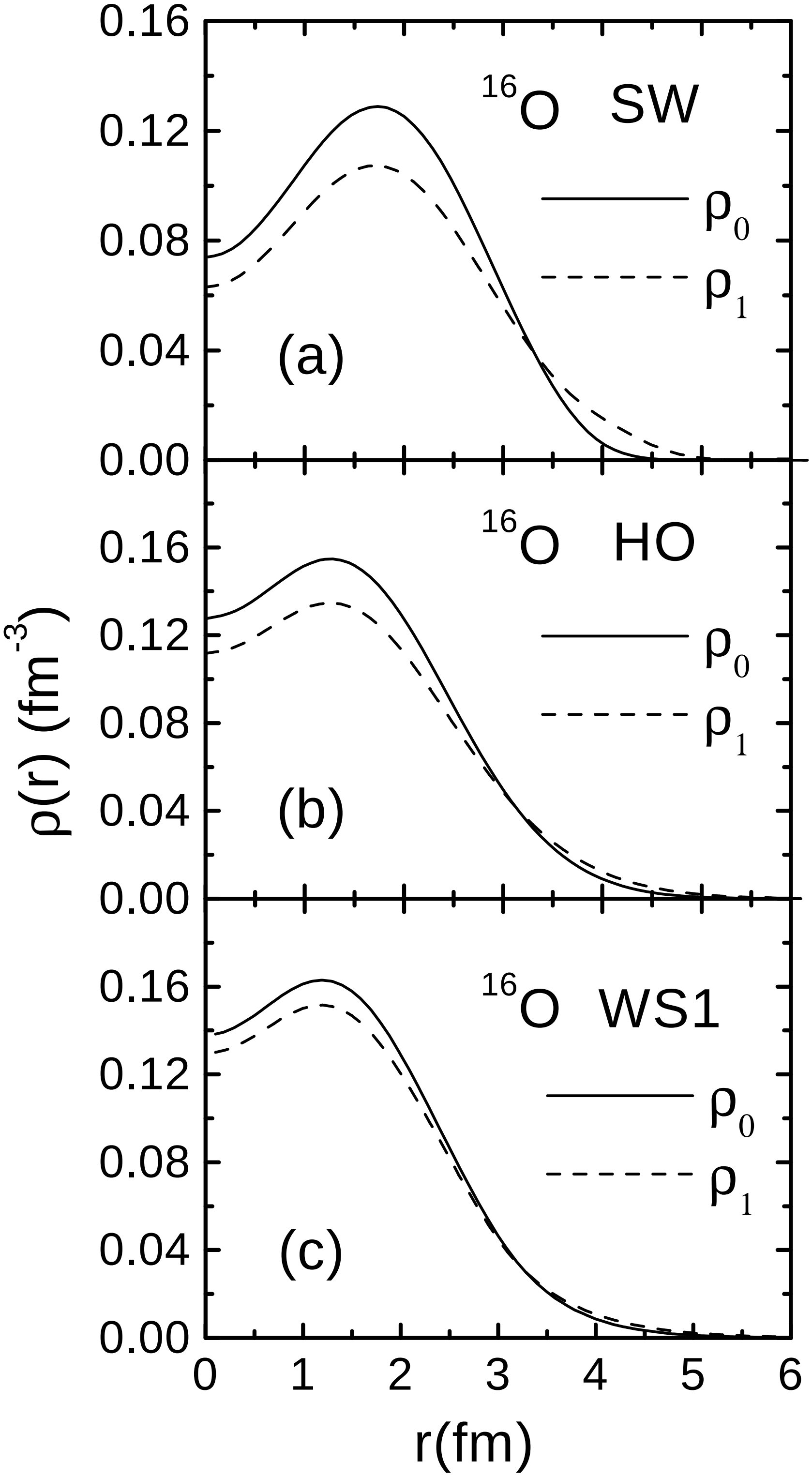

ρ(r) (fm^-3)
r(fm)
16O SW
16O HO
16O WS1
ρ0
ρ1
(a)
(b)
(c)
0.16
0.12
0.08
0.04
0.00
0
1
2
3
4
5
6

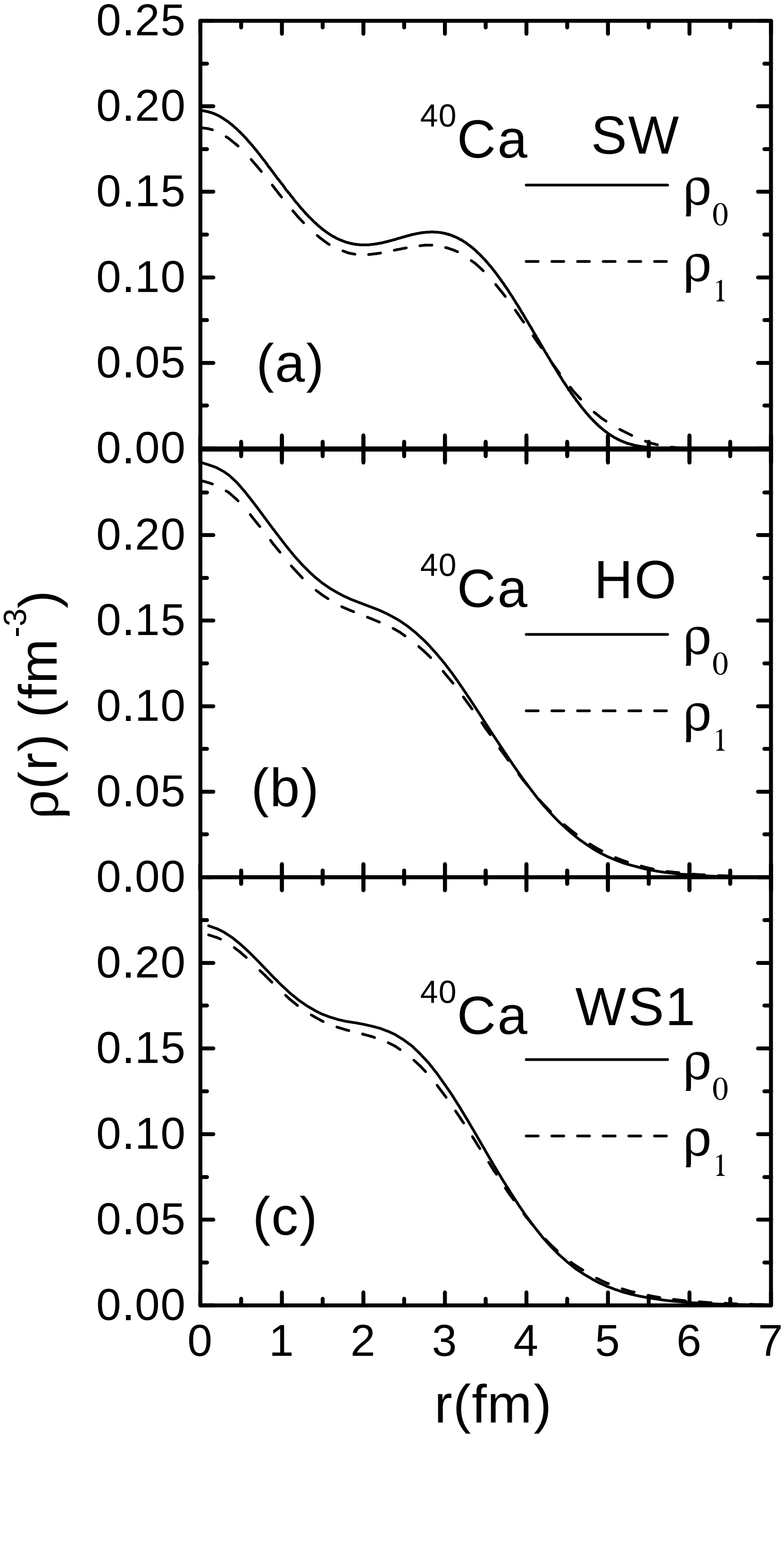

0.25
0.20
0.15
0.10
0.05
0.00
^{40}Ca SW
ρ_0
ρ_1
(a)
^{40}Ca HO
ρ_0
ρ_1
(b)
^{40}Ca WS1
ρ_0
ρ_1
(c)
ρ(r) (fm^{-3})
0 1 2 3 4 5 6 7
r(fm)

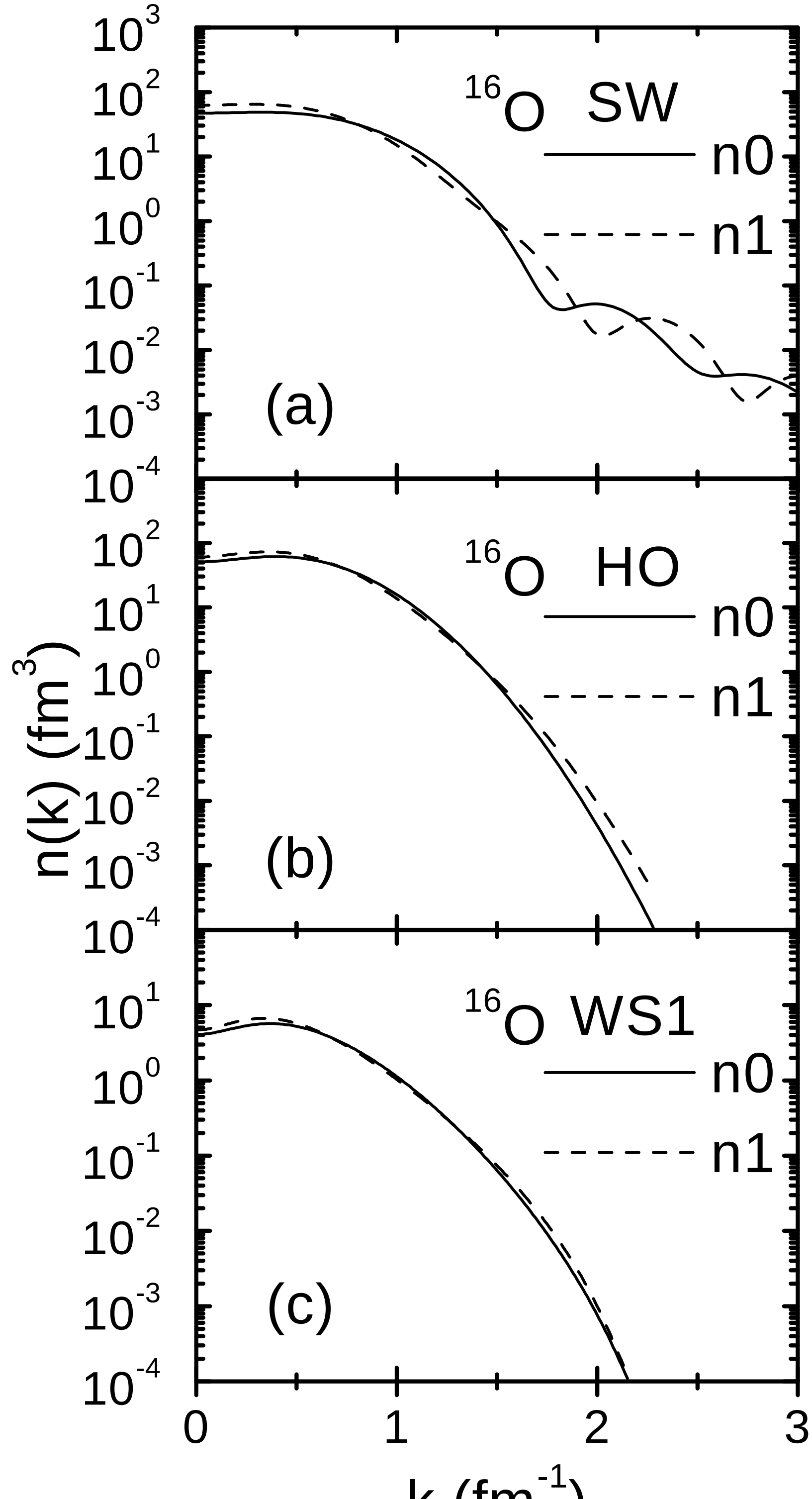

^{16}O SW
n0
n1
(a)
^{16}O HO
n0
n1
(b)
^{16}O WS1
n0
n1
(c)
n(k) (fm^3)
k (fm^{-1})

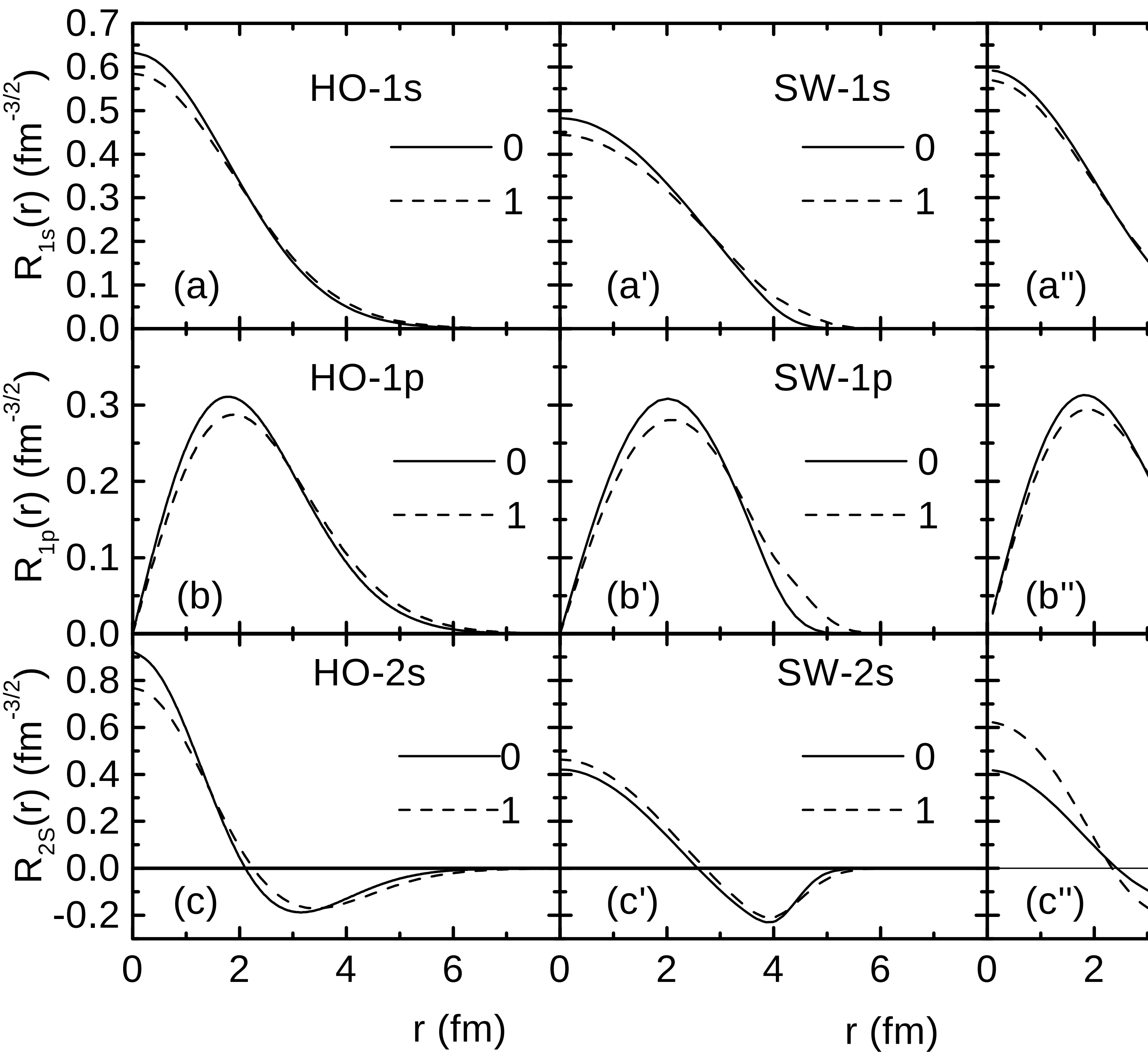

HO-1s
SW-1s
0
1
(a)
(a')
(a'')
HO-1p
SW-1p
(b)
(b')
(b'')
HO-2s
SW-2s
(c)
(c')
(c'')
$R_{1s}(r)$ (fm$^{-3/2}$)
$R_{1p}(r)$ (fm$^{-3/2}$)
$R_{2S}(r)$ (fm$^{-3/2}$)
r (fm)
r (fm)

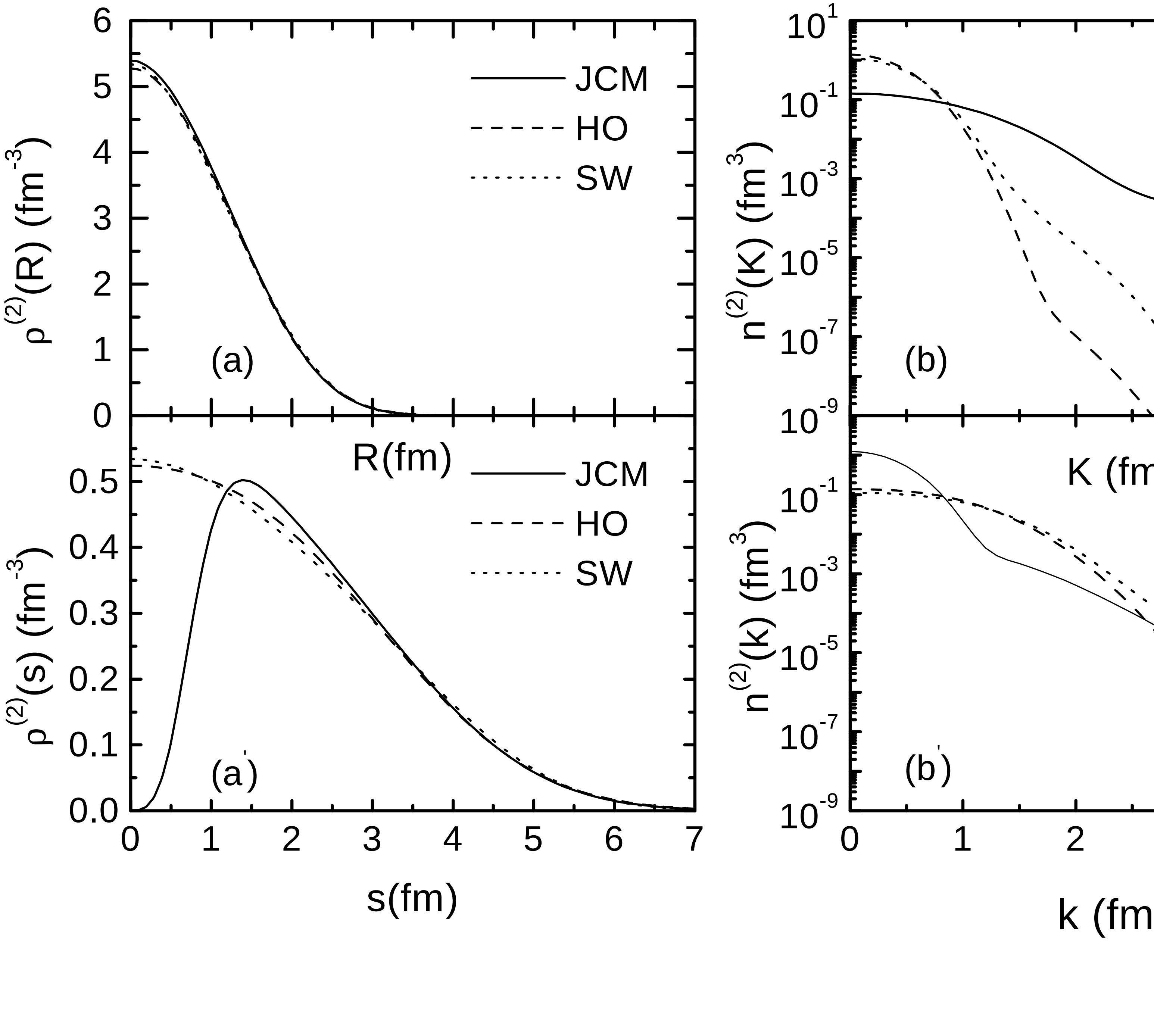

JCM
HO
SW
(a)
(a')
(b)
(b')
R(fm)
s(fm)
K (fm
k (fm